Electronic Supplementary Material (ESI) for Soft Matter.
This journal is © The Royal Society of Chemistry 2023

Rheological dynamics and structural characteristics of supramolecular assemblies of β-cyclodextrin and sulfonic surfactants

Bhargavi Bhat[a], Silabrata Pahari[a], Joseph Sang-Il Kwon[a,c] and Mustafa E. S. Akbulut[a,b,c]

[a.] *Artie McFerrin Department of Chemical Engineering, Texas A&M University, College Station, TX 77843, USA.*
[b.] *Department of Materials Science and Engineering, Texas A&M University, College Station, TX 77843, USA.*
[c.] *Texas A&M Energy Institute, College Station, TX 77843, USA.*

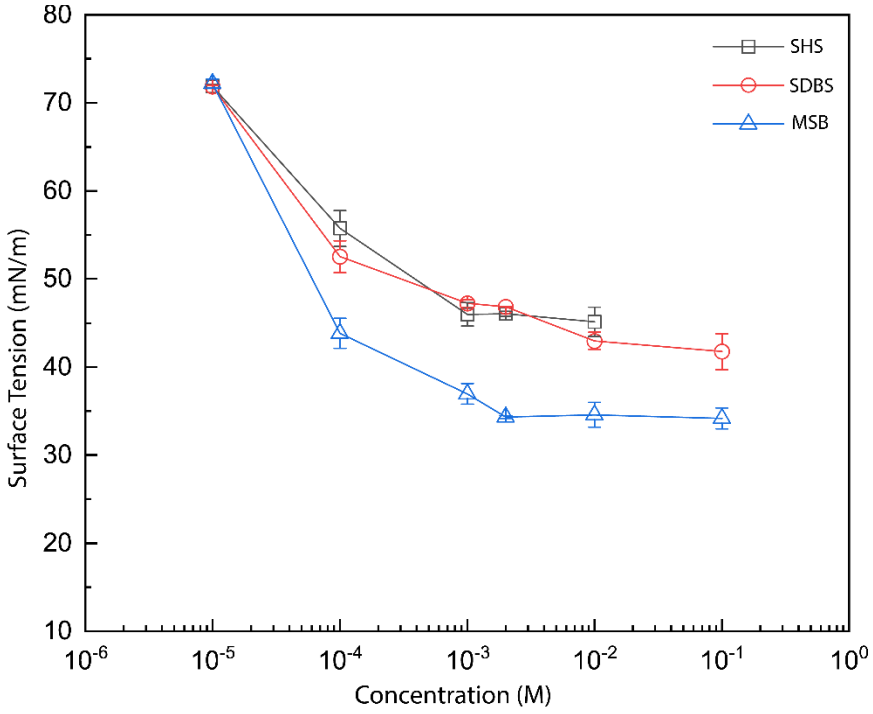

Figure S1: Surface tension curves for the amphiphiles used in the study.

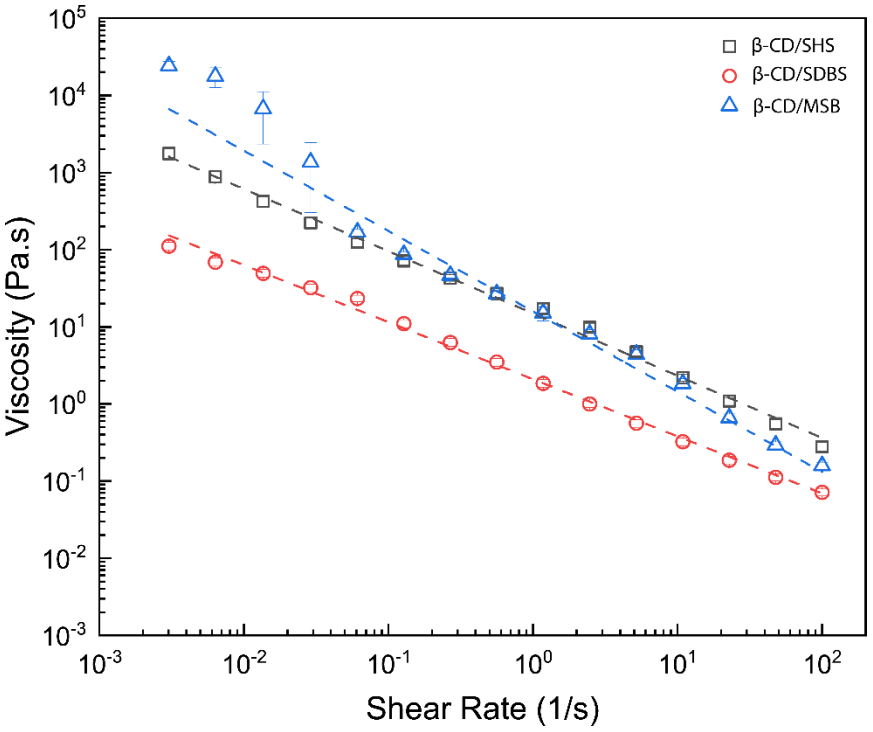

Figure S2: Fitting of β-CD/surfactant (2:1 molar ratio) suspensions to the power law equation.

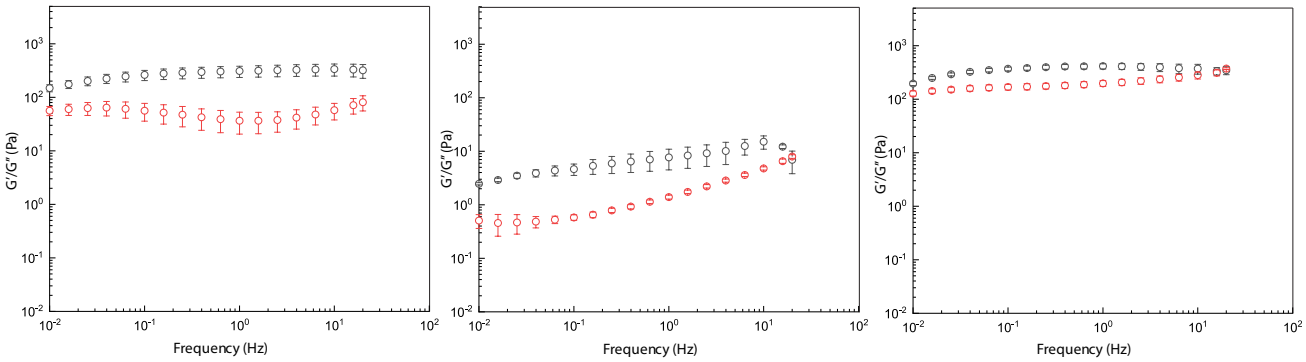

Figure S3: Storage(G')/Loss Modulus(G'') curves for β-CD/surfactant systems measured from 0.01-20 Hz. The concentration of surfactant is 50 mM and β-CD is 100 mM.

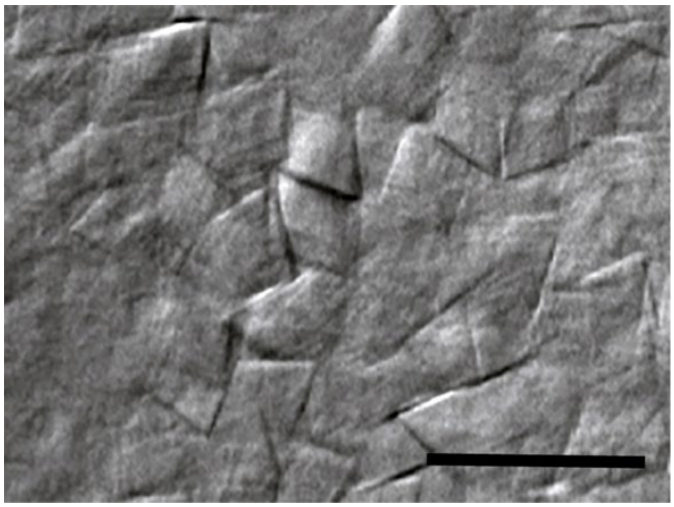

Figure S4: DIC optical micrograph at 63x of β-CD/SDBS. The scale bar is 10 μm.

Table S1: Table showing chemical shifts of H-3 and H-5 bonds of cyclodextrin for the various suspensions

Suspension	H-3 peak location	H-5 peak location	H-3 shift (δ_{H-3})	H-5 shift (δ_{H-5})
β-CD/MSB	4.6129	4.724	-0.1025	-0.1027
β-CD/SDBS	4.5655	4.7231	-0.0551	-0.1018
β-CD/SHS	4.6665	4.8697	-0.1561	-0.2484
Plain Cyclodextrin	4.5104	4.6213		

SAXS Analysis for the β-CD/surfactant systems

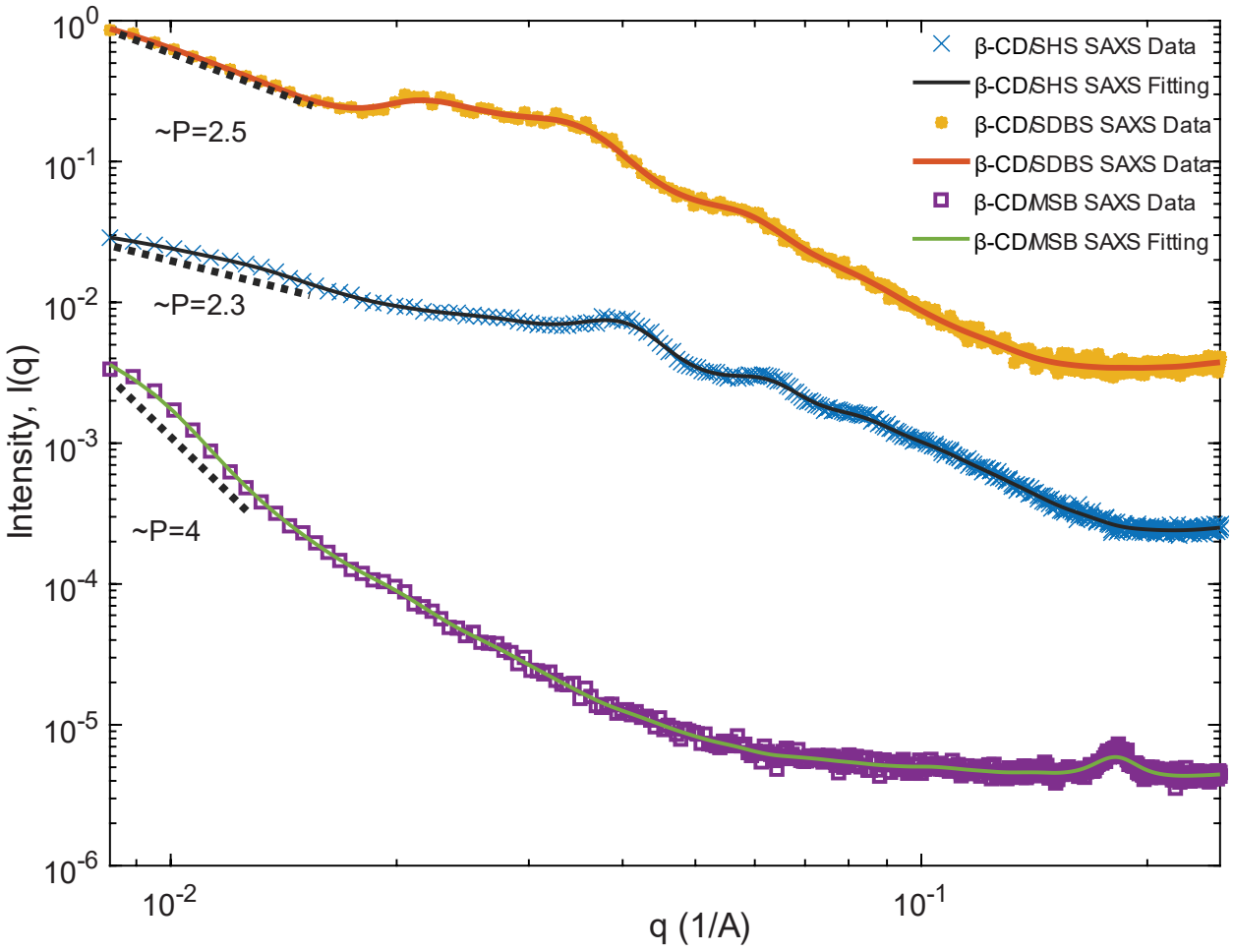

Figure S5: The SAXS analysis figure for different samples of β-CD/SHS, β-CD/SDBS and β-CD/MSB

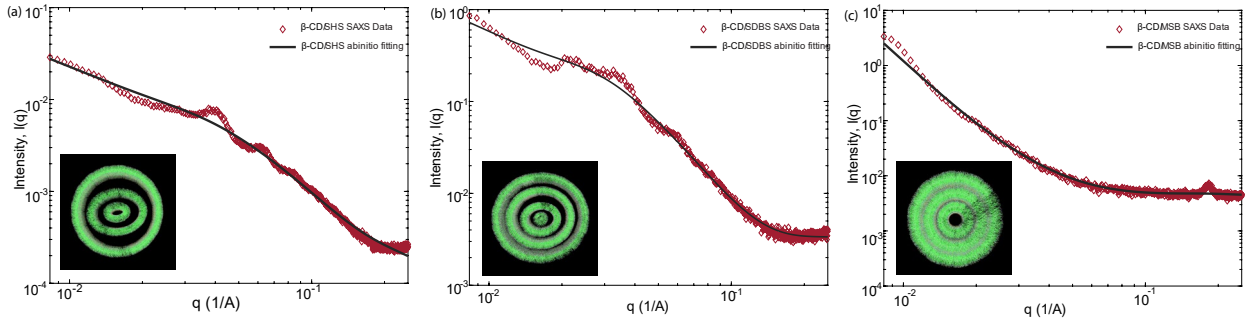

Figure S6: The results for ab-initio reconstructing of the SAXS profiles for three different samples, (a) β-CD/SHS (three tubular layers), (b) β-CD/SDBS (four tubular layers), and (c) β-CD/MSB (very tightly packed tubular structures)

β-CD/SHS: In the low q regime, there was a very small Guinea region followed by a power law decay with $P = 2.3$, this highlights the presence of mass fractals in the population[1]. On fitting the unified model to the low q regime, we obtain radius of gyration to be greater than 900 nm showing the presence of long tubules. The higher q regime was again fitted to four populations. These populations include three tubular regimes and one spherical regime. The mean diameter of the spherical particles was obtained to be 90 ± 10 nm [2]. The other three population of the tubular morphologies were obtained to be 40 ± 5 nm, 135 ± 10 nm, and 260 ± 15 nm respectively, the populations are considered to have gaussian distribution[3]. The ab-initio reconstruction of the SAXS profile and tuning the structural parameters with simulated annealing gives the result shown in Fig. S6(a). The figure highlights those three tubular structures layered on top of each other gives a reasonably good fit. The discrepancy in the ab-initio model and the SAXS data arises from assuming monodispersed tubules. The diameters of the stacked tubules were found to be 35 nm, 140 nm, and 250 nm respectively. We have assumed the diameter of the sphere to be that mean value obtained from fitting the population model, i.e 90 nm (this is also done for β-CD/SDBS).

β-CD/SDBS: There was a very small Guinea region observed followed by a power lay decay in the low q regime. On fitting the unified model to the low q regime, the radius of gyration was obtained to greater than 900 nm. This probably because there are significantly large nanostructures (long aggregated tubules). The power law decay shows the P=2.5, this behavior suggests the presence of mass fractals in the system [1]. Interpretation of this such a behavior is clear when analysis of the high-q regions is done. On fitting the high-q regions, we observed that 5 population models were required. There involved four cylindrical models and one spherical model in the intermediate regimes between 2×10^{-2} - 1.4×10^{-1}[2]. The mean diameter for the spherical particles was obtained to be 80 nm $\pm$ 15 nm (i.e, mean of 80 nm with a standard deviation of 15 nm). The four population for the cylindrical structures included a diameter of 20 ± 3 nm, 90 ± 15 nm, 180 ± 20 nm, and 240 ± 25 nm, the populations are assumed to have a gaussian distribution. The presence of mass fractals is a result of presence of the cylindrical and spherical particles. An ab-initio reconstruction of the structures leads to a probable morphology highlighted in Fig. S6(b). This figure shows that the ab-initio model of hollow tubular structures stacked over each other gives good fit. The diameter of the tubular structures obtained from simulated annealing are, 30 nm, 70 nm, 170 nm, and 230 nm respectively. It is important to realize that in the ab-initio

reconstruction we have assumed monodispersed particles which results in the discrepancy observed at certain points[3]. Furthermore, in the ab-initio reconstruction we have considered the size of sphere (which is not shown) to be that mean value obtained from fitting the population model, i.e 80 nm.

β-CD/MSB: The SAXS data for β-CD/MSB shows a small Guinea region observed followed by a power lay decay. On fitting the unified model to the low q regime, the radius of gyration was obtained to greater than 900 nm. These indicates the presence of long. The power law has a P=4, this shows the presence of smooth clear surfaces and absence of fractals[1]. This is important, when we fitted the high q data to population model we find that three tubular population having gaussian diameters distributions as $180 + 5$ nm, 120 ± 3.4 nm, and 70 ± 1.2 nm, were found to fit the data well[2]. A further validation of the analysis arises when we do the ab-initio reconstruction. This reconstruction gives us three bilayers stacked over each other very closely. By simulated annealing when we fit the structures, we get that the diameter of the monodisperse layers are 170 nm, 125 nm and 70 nm respectively[3]. The mismatch from the ab-initio reconstruction is very less and lowest as compared to any of the other two samples. This shows that the polydispersity is minimum for the β-CD/MSB samples and it has high volume fraction of the tubules. Furthermore, the layers are packed extremely tightly.

Limitations of the SAXS analysis and ab initio reconstruction of nanostructures have been highlighted in the work by Pahari et al. [3]. The primary challenge arises with the degeneracy of the structures that are generated via this ab initio method. In some cases, this degeneracy can be eliminated with molecular simulations that provide us with another metric, like potential energy which can allow us to reconstruct the unique morphology. In this study, we have used other characterization techniques like AFM, which shows the presence of tubules in the system. This observation gives us a degree of fidelity to the structures obtained from the SAXS analysis. Furthermore, it is to be noted that fitting the tightly packed hollow cylinders to the SAXS data gives a similar R^2 values as compared to the model of a solid cylinder. Distinguishing the solid cylindrical morphology and tightly packed cylindrical layers is challenging with only the SAXS method. Hybrid methods like combing SAXS data with molecular simulations can aid us to better addressing this challenge and also will be considered in future studies.

The SAXS analysis in this work is done in a two-fold fashion. First, the population models are fitted to the SAXS experimental data, and then the ab initio reconstruction of the three-dimensional nanostructures is done by fitting the models with polydispersity. For the ab initio reconstruction, first, the appropriate geometry that gives a reasonably good fit is chosen. Subsequently, simulated annealing is performed to fit the dimensions of the selected geometry to minimize the R^2 values. Once the best ab initio models are obtained, the SAXS profiles for the same model are fitted by introducing polydispersity. The introduction of polydispersity introduced a new set of parameters that are optimized with a nonlinear optimizer ipopt, and the optimal values that gives the best set of parameters are determined. On comparing the different geometries at the ab initio scale hollow tubules were found to give the best fit for SHS and SDBS. However, for MSB degeneracy exist in the solid cylinder and layered tubular structures that are packed very closely. This is an inherent limitation of the SAXS analysis and cannot be resolved without molecular simulations. In the case of SHS and SDBS the presence of a significant gap in between the tubules allows us to resolve those structures with higher fidelity.

References

[1] Beaucage G. Small-angle scattering from polymeric mass fractals of arbitrary mass-fractal dimension. J Appl Crystallogr 1996;29:134–46. https://doi.org/10.1107/S0021889895011605.

[2] Brosey CA, Tainer JA. Evolving SAXS versatility: solution X-ray scattering for macromolecular architecture, functional landscapes, and integrative structural biology. Curr Opin Struct Biol 2019;58:197–213. https://doi.org/10.1016/j.sbi.2019.04.004.

[3] Pahari S, Liu S, Lee CH, Akbulut M, Kwon JS il. SAXS-guided unbiased coarse-grained Monte Carlo simulation for identification of self-assembly nanostructures and dimensions. Soft Matter 2022;18:5282–92. https://doi.org/10.1039/d2sm00601d.